JPE 2-1-6

Neural Network Controller for a Permanent Magnet Generator Applied in Wind Energy Conversion System

Mona N. Eskander*

Electronics Research Institute, Cairo, Egypt

ABSTRACT

In this paper a neural network controller for achieving maximum power tracking as well as output voltage regulatio for a wind energy conversion system (WECS) employing a permanent magnet synchronous generator is proposed. Th permanent magnet generator (PMG) supplies a dc load via a bridge rectifier and two buck-boost converters. Adjusting th switching frequency of the first buck-boost converter achieves maximum power tracking. Adjusting the switchi frequency of the second buck-boost converter allows output voltage regulation. The on-time of the switching devices the two converters are supplied by the developed neural network (NN). The effect of sudden changes in wind speed and/ in reference voltage on the performance of the NN controller are explored. Simulation results showed the possibility achieving maximum power tracking and output voltage regulation simultaneously with the developed neural netwo controllers. The results proved also the fast response and robustness of the proposed control system.

Key Words: Wind energy conversion, Permanent magnet generator, Neural networks, Maximum power tracking

1.Introduction

Clean renewable energy sources such as solar and wind, have been developed over recent years. Wind is now on the verge of being truly competitive with conventional sources. A modern large electric wind energy conversion system (WECS) may generate up to 1.5 Mw. The cost, weight, and maintenance needs of mechanical gearing between the wind turbine and the electrical generator pose a serious limitation to the further increase in WECS power ratings. Direct coupled – low speed permanent magnet generators (PMG) are under development in response to this need. Permanent magnet excitation is favoured for developing new designs because of higher efficiency, high power densities, availability of high- energy permane magnet material at reasonable cost, and possibility rather smaller turbine diameter. Other advantages inclu the absence of brushes, slip rings, excitation windings, a excitation losses. For DC power generation, the lack excitation control is not a limitation for terminal volta and power control, since a diode rectifier and a dc- converter system, with various control strategies, perm load voltage and/ or load power control.

To achieve load voltage and power control usi conventional controllers, such as PID (Proportion Integral-Differential) controller, accurate mathematic models describing the dynamics of the system unc control is needed. This can be a limiting factor for syste with unknown varying dynamics. Even if a model can obtained for the system under control, unkno conditions such as disturbances, drifts, and noise may impossible to model with acceptable accuracy.

Nowadays, considerable attention has been focused o

Manuscript received November 1, 2001; revised January 30, 2002.

Corresponding Author: eskander@eri.sci.eg, Tel: +20-202-3310553, Fax: +20-202-3351631

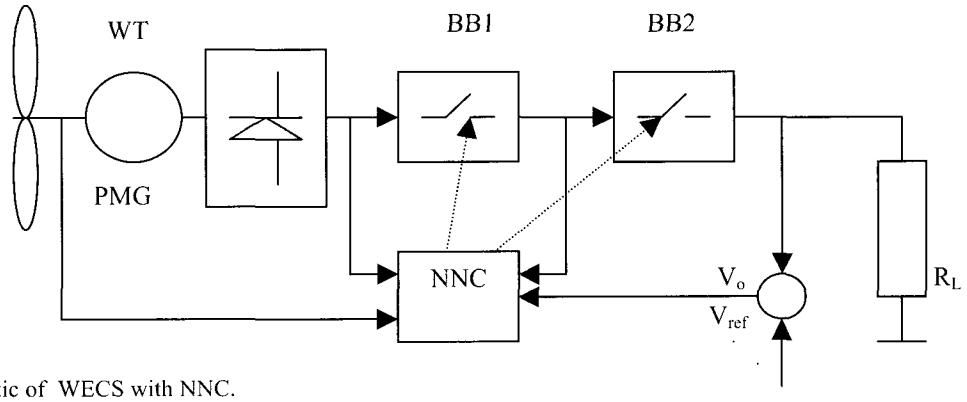

'ig. 1. Schematic of WECS with NNC.

he use of artificial neural network (ANN) in system nodeling and control applications[1-3]. The NN has several :ey features that make it suitable for controlling nonlinear ystems. These features include parallel and distributed ›rocessing, and efficient non-linear mapping between nputs and outputs without an exact system model. Also ⅣN's are characterized by the rapidity of response and obustness, which make them attractive to control wind :nergy conversion systems (WECS). However, in the field ›f generators, the application of NN has been developed ecently [4-8]. In [4] two NN systems were developed to egulate the output voltage of a turbo-generator. The first ⅣN was used for input output mapping, while the second ⅣN used for the voltage regulation. In [5], NN was used to levelop a saturation model for a synchronous generator. In 6] a NN observer was developed for on-line tracking of ;ynchronous generator parameters. In [7] NN was used for nodeling rotor parameters of a round rotor synchronous ;enerator. In [8] a NN was proposed to predict the naximum value of wind turbine coefficient C_p as function ›f the tip speed ratio λ and the blade angle, to maximize he power captured from the wind.

In this paper, a novel control strategy for maximum ›ower tracking (MPT) and output voltage regulation of a vind energy conversion system (WECS) employing a ›ermanent magnet generator (PMG) is proposed. The ³MG output is connected to a diode bridge rectifier ollowed by two buck-boost converters. A four neuron-nput, 8-neuron hidden layer, and two-neuron output layer ieural network controller (NNC) is developed to achieve wo goals. First, utilizing the maximum power available at :ach wind speed, (maximum power tracking), is achieved by adjusting the on-time of the switching device of the first converter BB1. Second goal is to regulate the load voltage by adjusting the on-time of the switching device of the the second converter BB2. The feasibility of the proposed NNC, is tested by allowing sharp changes in the wind speed as well as step up and down changes in the output reference voltage and deducing the NN's responses. Simulation results proved that the developed NNC enables MPT and output voltage regulation, within the whole wind speed range considered, with great accuracy. Results demonstrated the fast response, and robustness of the developed NNC in conjunction with the proposed WECS.

2. System Description and Modeling

The block diagram of the system adopted in this paper is shown in Fig. 1. It consists of a two - bladed, horizontal axis wind turbine coupled to a permanent magnet synchronous generator. An ac-dc power electronic interface with diode bridge rectifier and two dc-dc buck-boost converters are used for variable-speed operation of the wind generator supplying 110 dc voltage parallel loads. The system is designed to achieve maximum power tracking (MPT) and output voltage regulation within wide range of wind speed variation by means of a neural network controller (NNC). The NNC is designed with two outputs,namely; the on-time d_1 of the switching device of the first buck-boost converter (BB1), and the on-time d_2 of the switching device of the second buck-boost converter (BB2). The NNC is trained to adjust to d_1 to achieve MPT within a wide wind speeds range (3m/sec. to 8 m/sec.), and to adjust d_2 to achieve output voltage

regulation within the same wind speed range. The subsystems modeling are described as follows:

2.1 Wind Turbine (WT)

The wind turbine rotational shaft speed ω_m and the turbine power P_t at average wind velocity V_w (m/sec.), depend on the raduis of the turbine R (m) and its tip speed ratio λ given by [8]:

$$\lambda = \omega_m \frac{R}{V_w} \quad (1)$$

The power captured by the wind turbine is calculated as:

$$P_t = 0.5 C_p \rho A V_w^3 \quad (2)$$

where, ρ is the air density(kg./m^3), A is the turbine rotor cross section (m^2), and C_p is the power coefficient, which is a function of λ. It is subject to a fundamental upper limit of 16/27 derived from momentum theory and known as Betz limit.

To make an optimal use of the available wind power, it is necessary to change the turbine speed ω_m in proportion to the wind speed V_w, to hold λ at the value for maximum C_p as the wind speed varies. The power P_t versus rotational turbine speed at different wind speeds for the two-bladed rotor, blade-pitch regulated, 1.6Kw wind turbine adopted in this work, is shown in Fig. 2 .On the same figure, the maximum power line P_{max} at different speeds is plotted. The maximum power transfer from the wind is achieved by ensuring the operation along the curve given by P_{max} in Fig. 2. To deduce the maximum available wind power at each wind speed, an equation relating the maximum turbine power with the rotational turbine speed is derived from the characteristic curve shown in Fig. 2 by interpolation. The interpolation resulted in the following equation for maximum wind power as function of ω_m:

$$P_{max} = 0.0005\,\omega_m^3 - 0.00125\,\omega_m^2 + 0.7\,\omega_m - 74.6 \quad [W] \quad (3)$$

2.2 The Permanent Magnet Synchronous Generator (PMG)

A 2.25Kw, 24pole, 500rpm rated speed, permanent magnet generator (PMG), is selected for the direct drive proposed application. The generator output voltage varies

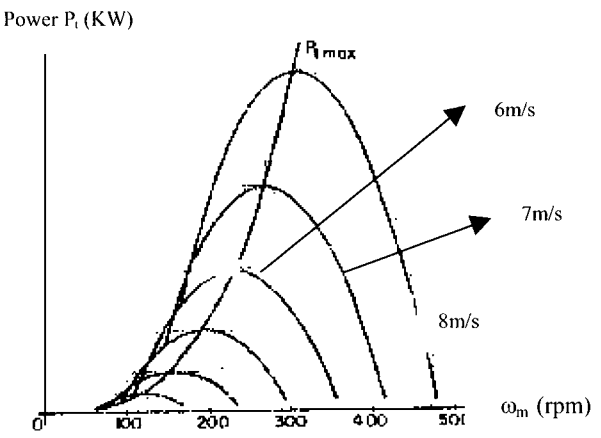

Fig. 2. Turbine Power-Speed Characteristics.

according to the wind speeds variation. Hence, the 3-phas output of the PMG is rectified with a full wave diod bridge rectifier, filtered to remove significant rippl voltage components, and fed to two consecutive dc-d buck-boost converters. For an ideal PMG, the line to lin voltage is given as:

$$V_L = K_V\ \omega \sin \omega_e t \quad [V] \quad (4$$

where, K_v is the voltage constant and ω_e is the electric frequency related to the mechanical speed ω_m by:

$$\omega_e = \omega_m \left(\frac{2}{n_p}\right) \quad [rad./sec.] \quad (5$$

where, n_p is the number of poles of PMG.

Including commutation delays, the dc rectifier voltag V_d is given as:

$$V_d = \frac{(3\sqrt{2})}{\pi} V_{Lrms} - \frac{3\omega_e L_s}{\pi} I_d \quad [V] \quad (6$$

where, V_{Lrm} is the rms value of the PMG output voltag I_d is the rectifier output current, and L_s is the stat inductance.

Neglecting the generator and rectifier losses, the PM output rectified electrical power P_{dc}, is equal to th mechanical power input to it. Hence, for maximum pow extraction, P_{dc} is set equal to P_{max} and is calculated as:

$$P_{dc} = P_{max} = V_d\ I_d \quad (7$$

The value of P_{dc} is forced to follow P_{max} by adjustin

the on time of the switching device of the first buck-boost converter (BB1).

2.3 Buck-Boost Converters

Two buck-boost converters are employed in the proposed system. The converters are chosen due to their ability of output voltage regulation from higher or lower input voltage values [9]. Fig. 3 shows the basic buck boost converter circuit diagram. The state- space averaging method is used for analyzing the switching circuit performance. Assuming continuous current in the buck-boost inductor, the averaging method is applied. For each of the two buck-boost converters employed in the proposed system, state variables X_1 and X_2 are chosen as the inductor current, X_1, and the capacitor voltage, X_2. The switching period is T, and the on-time of the switching device is d. Hence for the shown circuit the state equations during switch on, i.e. the dT interval, are:

$$U = L\,(p\,X_1) \tag{8}$$

$$0 = C\,(p\,X_2) + X_2/R \tag{9}$$

where, p=d/dt, and U is the input dc voltage to the converter. for BB1 $U=V_d$, while for BB2, U=output voltage of BB1.

During the (1-d) T interval, the state space equations is:

$$L\,(p\,X_1) = X_2 \tag{10}$$

$$-X_1 = C\,(p\,X_2) + \frac{X_2}{R} \tag{11}$$

Applying state space averaging, the state coefficient matrix, A, is:

$$A = \begin{vmatrix} 0 & \dfrac{(1-d)}{L} \\ \dfrac{-(1-d)}{C} & \dfrac{-1}{RC} \end{vmatrix} \tag{13}$$

State- space averaged source coefficient matrix is:

$$B = \begin{vmatrix} d/L \\ 0 \end{vmatrix} \tag{14}$$

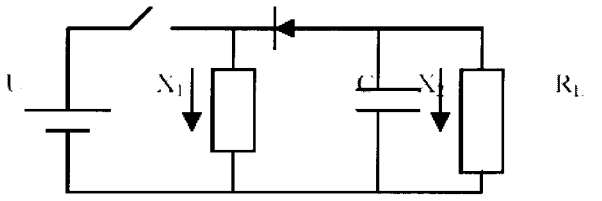

Fig. 3. Ideal Buck-Boost Converter.

Hence, the two nonlinear state-space-averaged equations are:

$$p\,X_1 = \frac{(1-d)}{L\,(X_2)} + \frac{d}{L\,U} \tag{15}$$

$$p\,X_2 = \frac{-(1-d)}{C\,(X_1)} - \frac{X_2}{R\,C} \tag{16}$$

2.3.1 First buck-Boost Converter (BB1)

For the first converter BB1, the on-time of the switching device d_1, is varied to achieve maximum power tracking at variable wind speeds. The parameters of BB1 are defined by the suffix '1'. Hence in equations 15 and 16 BB1 parameters are substituted for by:
$U= U_1= V_d$, $C = C_1= 10$ mF, $X_1 = L_1= 10$ mH, X_2 = output voltage of BB1, and R_L is the equivalent input resistance of the second buck boost converter BB2 as seen by BB1.

2.3.2 Second Buck-Boost Converter (BB2)

The parameters of BB2 are given suffix '2'. The on-time, d_2, of the switching device, is varied to achieve output voltage regulation within the wind speeds range considered in this work (from 3 m./sec. to 8 m./sec.). The parameters of BB2 in equations 15 and 16 are:

U_2=output dc voltage of BB1, $C = C_2= 10$ mF, $X_1 = L_2= 10$ mH, X_2 = output voltage of BB2, and R_L = the load resistance

3. Control Strategy

Under steady state operation, (p=d/dt=0), the equations of the generator, the rectifier, the average of the states of the first buck-boost converter (BB1), and the average of the states of the second buck-boost converter (BB2) (equations 4-7,15-16) are manipulated to achieve the two goals of this research:

(i) Maximum power tracking, achieved by varying the

on-time (d_1) *of the switching device of the first buck-boost converter (BB1).*

(ii) Regulation of the output voltage of the conversion system, achieved by varying the on-time (d_2) of the switching device of the second buck-boost converter (BB2).

Manipulating these equations, and setting d_1^* as the switching time allowing MPT, and d_2^* as the switching time that enables output voltage regulation, leads to the following expressions for (d_1^*), and (d_2^*):

$$d_1^* = \frac{Z}{(1+Z)} \tag{17}$$

where,

$$Z = \left[\left(\frac{R_L}{2P_{max}}\right)\right]^{\frac{1}{2}} V_{rms} + \left[\left(\frac{(R_L V_{rms}^2)}{2P_{max}\omega_e^2 L_s^2}\right)\right]^{\frac{1}{2}} - \left[\frac{\pi R_L}{3\omega_e L_s}\right]$$

and,

$$d_2^* = \frac{y}{(1+y)} \tag{18}$$

where,

$$y = \left(\frac{V_{ref}}{P_{max}}\right)\left[\left(\frac{\sqrt{2}V_{Lrms}}{\omega_e L_s}\right) + \left(\frac{V_{Lrms}^2}{2\omega_e^2 L_s^2}\right)^{\frac{1}{2}} - \left(\frac{\pi P_{max}}{3\omega_e L_s}\right)^{\frac{1}{2}}\right]$$

4. Neural Network Structure

4.1 NN Learning Strategy

A basic component of a neural network is described by a set of interconnected weights (w_{ij}) a node activation function, F, and a bias (θ_i). In this description, the output, a_i of the ith element of the network is determined by mapping of the effective input, x_i, through an activation function at element. The output of each basic processing element can be determined by different activation functions. A convenient choice for the activation function is the sigmoidal function given below:

$$a_i = F(\chi) = sigm(\chi) = \frac{1}{(1+e^{\chi})}$$

In order to establish the neural network model, the interconnected weights (w_{ij}), and biases (θ_i), are trained according to the existing input/output patterns. The process is intended to minimize the error between the network outputs ($d^p{}_i$) and the actual outputs ($a^p{}_i$), for the same inputs. By defining the error measure, E^p, as the total quadratic error for pattern p at N_o output units, i.e.:

$$E^p = 0.5 \sum_{i=1}^{No} \left(d_i^p - a_i^p\right)^2 \tag{19}$$

The learning process is to adjust the weights and biases based on the training pattern p to minimize the error measure E^p, in a gradient descent manner. It is clear that if the error measure is minimized for all patterns, the overall measure is also minimum. Due to the analytic nature of the sigmoidal activation function adopted here the error minmization process can be backwardly traced from the output layer towards the hidden layer. As a result using an iterative procedure, called the generalized delta rule, the adjustment of the network weights and biases for minimizing E^p is obtained.

4.2 Neural network Controller (NNC) Model

One of the important aspects of applying a NN to any particular problem is to formulate the inputs and outputs of the NN structure under study. The proposed control scheme, imposing maximum power tracking and output voltage regulation, dictates the outputs of the NN controller. The NN controller is designed to give two outputs; these are d_1^* and d_2^*, as given by equations 17 and 18.

Off line training for the proposed NNC was applied. Data for off-line training can be obtained either by simulation or experiment. For this present work, the data is obtained by simulating the proposed WECS in open-loop system. The simulation is carried out at random wind speeds, and different values of reference voltage. Following the control strategy, described in section 3 of this paper, d_1^* and d_2^* are calculated, which present the targets of the NN controller.

After many trials, the developed NNC, shown in Fig. 4, eventually employed a 4-neurons input layer, an 8-neurons hidden layer, and a 2-neurons output layer. The input network parametrs are:

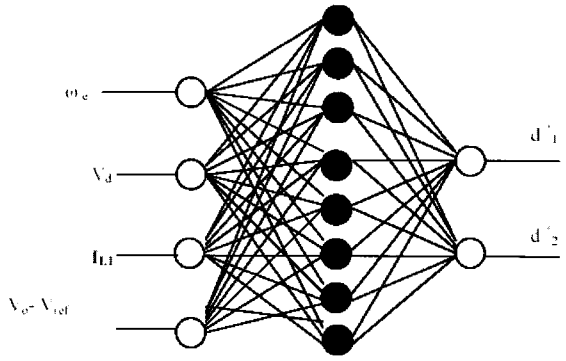

Fig. 4. Neural Network Controller Structure.

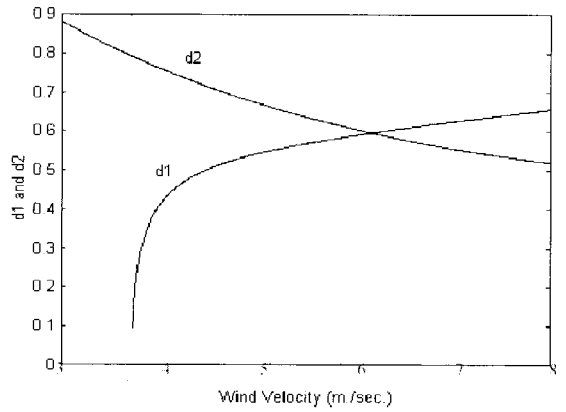

Fig. 5. Variation of d1 and d2 for maximum power tracking and output voltage regulation.

the generator speed ω_e, the rectifier output voltage V_d, the inductance current of the first converter I_{L1}, and the difference between the actual output voltage and the reference output voltage V_{ref}.

For the present work, such NNC structure gave satisfactory results with small number of neurons, hence better in terms of memory and time required to implement the NN in control. The transfer function used in the input and hidden layers are the sigmoid, while purellin transfer function is used for the output layer. The training process has been carried out during 1000 epochs, using 6000 input-output patterns. It was designed for achievement of maximum power tracking and voltage regulation of the proposed WECS.

5. Simulation Results

To evaluate the performance of the NN controlled WECS proposed in this paper, the values of d_1^* and d_2^* necessary to track maximum power available in the wind

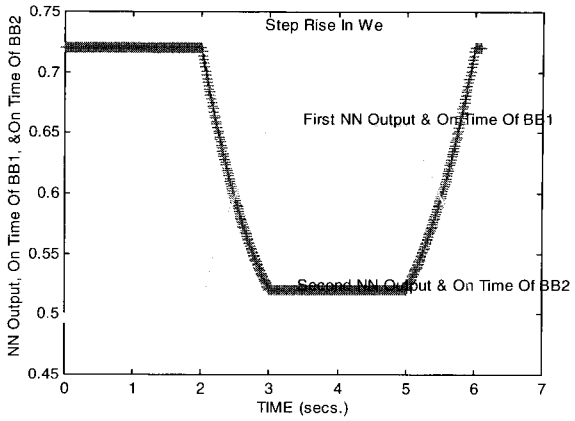

Fig. 6. NNC outputs and target outputs following step rise i shaft speed.

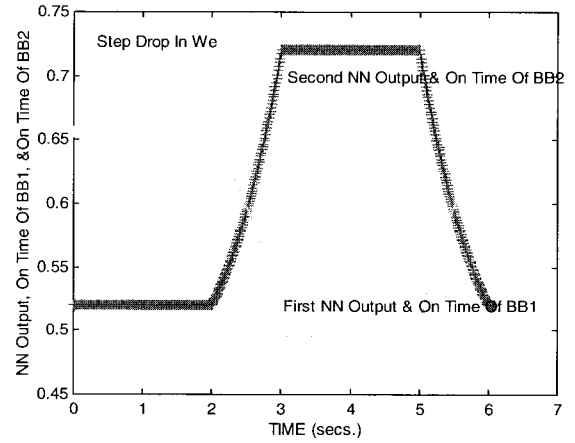

Fig. 7. NNC outputs and target outputs following step drop i shaft speed.

and to regulate output voltage are first calculated from simulation program. These values are shown in Fig. 5 a function of wind speed. The next step is to evaluate the performance of the developed NN controller. This is done by exciting the proposed wind generation system with sudden sharp changes in wind speed and step up and down changes in reference voltage and deducing the NNC outputs responses following these variations.

Simultaneous abrupt changes in the wind speed and step change in the reference voltage are also applied and NNC response plotted.

Fig. 6 shows the two outputs of the proposed NNC following a step rise of 50 rpm in shaft speed coresponding to change in wind speed, at constant reference voltage. On the same figure, the values of d_1^* and d_2^* required to achieve the two goals of the proposed

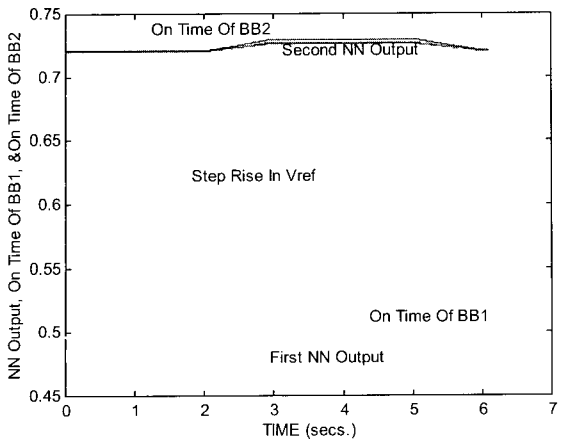

Fig. 8. NNC outputs and target outputs following step rise in reference voltage.

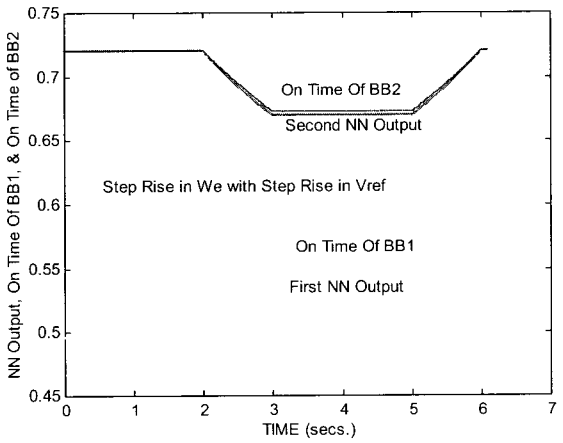

Fig. 9. NNC outputs and target outputs following step rise in shaft speed with step rise in reference voltage.

system, i.e. the targets, are also shown. The trivial differences between the NNC actual outputs and the targets prove that the proposed controller accurately tracks the targets without overshooting.

Fig. 7 shows the two outputs of the proposed NNC after a sudden drop of 50 rpm in the shaft speed at constant reference voltage. On the same figure, the values of d_1^* and d_2^* required to achieve the two goals of the proposed system are also shown. It is clear that the NNC outputs coincide with the targets, thus proving the accuracy and fast response of the controller.

Fig. 8 shows the response of the proposed NNC before and after a step rise in the reference voltage from 110 to 150 volts for a time interval of 3 units, at constant wind speed. Accurate tracking of NNC to reference voltage with maximum power capturing is obvious.

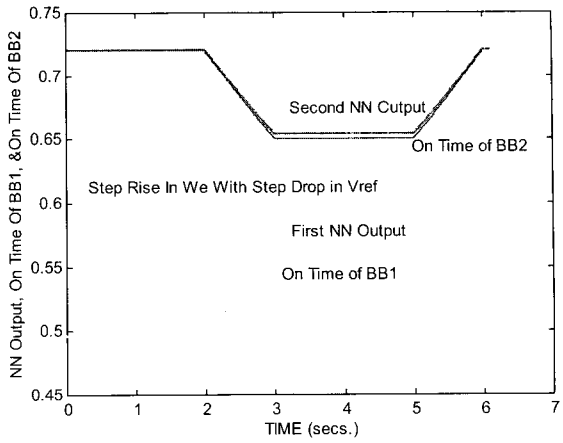

Fig. 10. NNC outputs and target outputs following step rise in shaft speed with step drop in reference voltage.

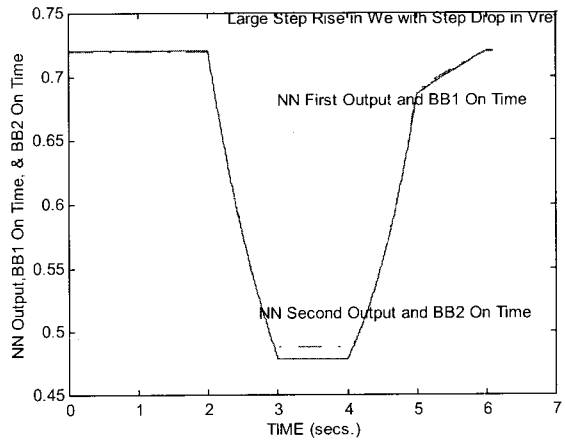

Fig. 11. NNC outputs and target outputs following large step rise in shaft with step drop in reference voltage.

The NNC outputs following simultaneous step rise in wind speed (50 rpm) and step rise in V_{ref}(40 V.) are shown in Fig. 9. Comparing these outputs with the values of d_1^* and d_2^* required to achieve the two control system goals proves the validity of the developed NNC under such complicated variation. Such accurate tracking is also shown in Fig. 10, where a step rise of speed (50 rpm) is allowed with a step drop in V_{ref}(40 V step).

In Fig. 11, the feasibility of the NNC is further tested by comparing its output after high rise in shaft speed (100 rpm) simultaneous with a step drop in V_{ref} (40 V step) with values of d_1^* and d_2^* required to achieve the two goals. The figure demonstrates the accurate tracking of the controller to the system targets. Similar results are obtained in Fig. 12 where high rise in speed (100 rpm) is allowed simultaneously with a step rise in V_{ref}(40 V step).

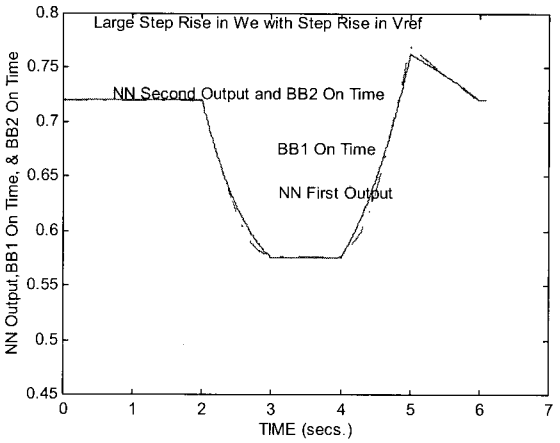

Fig. 12. NNC outputs and target outputs following large step rise in shaft speed with step rise in reference voltage.

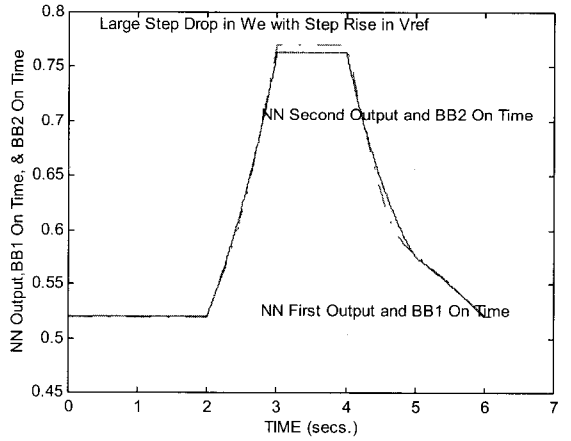

Fig. 13. NNC outputs and target outputs following large step drop in shaft speed with step rise in reference voltage.

In Fig. 13 NNC outputs under large step drop in the shaft speed (100 rpm), simultaneous with a 40 volts step rise in V_{ref} are compared with the system targets (d_1^* and d_2^*) required to achieve the two control system goals. Both results further proves the accuracy and feasibility of the developed NNC.

The system is designed so that for a rise in wind speed, leading to a rise in the output power, excess power than load demand is stored in a battery bank. While for a decrease in wind speed, leading to decrease in power than load demand, load is supplied from batteries.

6. Conclusion

In this paper the feasibility of a neural network controller developed for achieving maximum power tracking as well as output voltage regulation, for a win energy conversion system (WECS) employing permanent magnet synchronous generator, is tested. Th PMG output is connected to a diode bridge rectifie followed by two buck-boost converters. The propose control strategy aims at achieving two goals: first, t utilize the maximum power available from the wind, i.e allow maximum power tracking, the on-time d^*_1 of th switching device of the first converter BB1 is varied t follow variation in wind speeds. Second goal is to regulat the load voltage by adjusting the on-time d^*_2 of th switching device of the second converter BB2. A fou neurons-input, 8-neurons hidden layer, and two-neuron output layer neural network controller (NNC) is develope to achieve the two goals implied by the control strategy The feasibility of the proposed NNC, is tested b simulating sharp changes in the wind speed as well as ste up and down changes in the output reference voltage an deducing the NNC outputs response. The validity of th developed NNC is also proved by applying simultaneou variation in the shaft speed and in the reference voltage and deducing the NNC outputs response. Results prove the accuracy of the developed NNC, its fast response an robustness. The relatively small number of neurons offer a simple way of implementing the controller.

Appendix

Wind Turbine parameters:

2-bladed, pitch- regulated, 1.6 Kw, raduis=2m.

Permanent magnet generator parameters:

2.25Kw, 24 pole, 500rpm rated speed

Ls=1.29 mH, Rs=1.5 ohm, Kv=1.2 v/rpm

References

[1] M.A. El-Sharkawi and S. Weerasooriya, "Developmen and implementation of self-tuning tracking controller fo dc motors", IEEE Trans. on EC, Vol. 5, No. 1, pp. 122 ~ 128, 1990.

[2] S. Weerasooriya and M.A. El-Sharkawi, "Identificatio and control of a dc motor using back-propagation neura networks", IEEE on EC, Vol. 6, No. 4, pp. 663 ~ 669 1991.

[3] T. Fukuda and T.Shibata, Theory and applications o neural networks for industrial control systems, IEEE on IE

vol. 39, No., pp. 472~489, 1992.

[4] Q.H. Wu, B. Hogg, and G.Irwin, "A neural network regulator for turbogenerators", IEEE Trans. On NN, vol. 3, No. 1, pp. 95~100, 1992.

[5] H. Tsai, A. Kehanyi, J. A. Demcko, and D. Selin, "Development of a neural network based saturation model for synchronous generator analysis", IEEE Trans. On EC, Vol. 10, No. 4, pp. 617~624, 1995.

[6] S. Pillutla, A. Keyhani, and I. Kamwa, "Neural Network Observers for on-line tracking of synchronous generator parameters", IEEE Trans. On EC, vol. 14, No. 1, pp. 23~30, 1999.

[7] S. Pillutla, and A. Keyhani, "Neural network based modeling of round rotor synchronous generator rotor body parameters from operating data", IEEE Trans. On EC, Vol. 14, No. 3, pp. 321~327, 1999.

[8] R. Chedid, F. Mrad, and M. Basma, "Intelligent control of a class of wind energy cinversion systems", IEEE Trans. On EC, Vol. 14, No. 4, pp. 1597~1604, 1999.

[9] Yim-Shu-Lee, "Computer aided analysis and design of switch mode power supplies", Marcel Dekker Inc. 1993.

Mona Naguib Eskander obtained the M.Sc and Ph.D degrees in Electrical Engineering from Egypt. She is currently an associate professor in the Power Electronics and Energy Conversion Dept. in the Electronics Research Institute of Cairo, Egypt.

Her practical experience is in the field of digital triggering and control circuits. Her current researches include; control of electrical drives, renewable energy generation systems (wind, PV, and Fuel Cell systems) control of robot manipulators and application of artificial intelligence (Fuzzy logic and Neural Networks) in control of electrical machines. She is a member in a joint project with industry to design and construct a spray painting robot.